Chapter 4

Combining the Models

4.1 The Numerical-Integration Scheme

The approach followed in the thesis is to treat the flowing air, the structure, and the devices of the control system as elements of a single dynamical system, and to integrate all of the governing equations numerically, simultaneously, and interactively in the time domain. There is a fundamental complication with the time-domain approach chosen to solve the aeroelastic problem: to predict the aerodynamic loads one must know the motion of the structure, and to predict the motion of the structure one must know the aerodynamic loads. To overcome this complication, an iterative scheme that accounts for the interaction between the aerodynamic loads and the motion of the structure was developed. The procedure is based on Hamming's fourth-order predictor-corrector method (Carnahan et al. [181]). This scheme was chosen for two reasons (1) the aerodynamic model functions better when the loads are only evaluated at integral time steps, and (2) the aerodynamic loads contain contributions that are proportional to the acceleration (the so called added-mass effect). These contributions come from $\dfrac{\partial \Phi}{\partial t}$, where $\Phi(\mathbf{R}, t)$ is the velocity potential in Bernoulli's equation; $\Phi(\mathbf{R}, t)$ is proportional to the velocity. For both reasons, Runge-Kutta-type methods are not suitable, but predictor-corrector methods, using iteration, can treat acceleration on both sides of the equations of motion, and they do not evaluate the loads at fractions of the time step. It turns out that the present numerical scheme, with some further adaptations and innovations, is also ideally suited for ship-dynamics problems.

The equations of motion for the structures, Equations (3.26), (3.35) and (3.36), (3.44) and (3.45), and (3.66)-(3.69), can be written as a system of $2n$ first-order ordinary-differential equations (where $n = 7$ for the wing, $n = 2$ for bridges one and two, and $n = 4$ for bridge three):

$$\dot{\mathbf{y}}(t) = \mathbf{F}[\mathbf{y}(t)] \tag{4.1}$$

in this equation half of the vector $\mathbf{F}$ represents generalized velocities and the other half represents generalized forces divided by the corresponding inertias. In general the loads depend explicitly on $\mathbf{y}$, and implicitly on the history of the motion and the acceleration through the term $\frac{\partial \Phi}{\partial t}$, as we saw in the previous two chapters.

In Equation (4.1) $\mathbf{F}[\mathbf{y}(t)] = \{F_1[\mathbf{y}(t)], F_2[\mathbf{y}(t)], \ldots, F_{2n}[\mathbf{y}(t)]\}^T$, $\mathbf{y}(t) = [y_1(t), y_2(t), \ldots, y_{2n}(t)]^T$, and $\dot{\mathbf{y}}(t) = \frac{d}{dt}\mathbf{y}(t)$ are $(2n \times 1)$ vectors. The details of the basic numerical procedure used to determine the current value of the vector $\mathbf{y}$ are given next:

1. Let $t_j = j\Delta t$ denote the time at the j-th time step, where Δt is the time-step size used to obtain the numerical solution, and

$$\mathbf{y}^j = \mathbf{y}(t_j) \tag{4.2}$$

$$\dot{\mathbf{y}}^j = \dot{\mathbf{y}}(t_j) \tag{4.3}$$

$$\mathbf{F}^j = \mathbf{F}[\mathbf{y}(t_j)] \tag{4.4}$$

2. At t_0 (i.e., $t = 0$) we have the initial conditions of the problem, i.e. we know $\mathbf{y}^0 = \mathbf{y}(t_0)$. Hence, using Equation (4.1) we obtain the value of $\dot{\mathbf{y}}^0$ as:

$$\dot{\mathbf{y}}^0 = \mathbf{F}^0 = \mathbf{F}\left(\mathbf{y}^0\right) \tag{4.5}$$

3. At t_1 (i.e., $t = \Delta t$) the *predicted* solution, ${}^p\mathbf{y}^1$, is computed by the *Euler Method*

$${}^p\mathbf{y}^1 = \mathbf{y}^0 + \Delta t\ \mathbf{F}^0 \tag{4.6}$$

4. The predicted solution is corrected by using the *Modified Euler Method*

$$ {}^{k+1}\mathbf{y}^1 = \mathbf{y}^0 + \frac{\Delta t}{2} \left({}^{k}\mathbf{F}^1 + \mathbf{F}^0 \right) \tag{4.7} $$

where k is the iteration number, and

$$ {}^{k}\mathbf{F}^1 = \mathbf{F}\left({}^{k}\mathbf{y}^1 \right) \tag{4.8} $$

where ${}^{1}\mathbf{y}^1 = {}^{p}\mathbf{y}^1$.

5. The previous step is repeatedly applied until the iteration error

$$ e^1 = \left\| {}^{k+1}\mathbf{y}^1 - {}^{k}\mathbf{y}^1 \right\|_\infty \tag{4.9} $$

is less than a prescribed error tolerance ϵ.
Here the ℓ_∞-norm of a vector $\mathbf{x} = (x_1, x_2, \ldots, x_n)^T$ is defined by

$$ \|\mathbf{x}\|_\infty = \max_{1 \le i \le n} |x_i| \tag{4.10} $$

If $e^1 > \epsilon$ then we set

$$ {}^{k}\mathbf{y}^1 = {}^{k+1}\mathbf{y}^1 \tag{4.11} $$

$$ {}^{k}\dot{\mathbf{y}}^1 = {}^{k+1}\dot{\mathbf{y}}^1 \tag{4.12} $$

and go to Equation (4.7); if $e^1 \le \epsilon$ then we set

$$ \mathbf{y}^1 = {}^{k+1}\mathbf{y}^1 \tag{4.13} $$

$$ \dot{\mathbf{y}}^1 = {}^{k+1}\dot{\mathbf{y}}^1 \tag{4.14} $$

and compute the response at $t_2 = t_1 + \Delta t$.

6. At t_2 (i.e., $t = 2\Delta t$) the *predicted* solution, ${}^{p}\mathbf{y}^2$, is computed by the *Adams-Bashforth*

Two-Step Predictor Method

$$ {}^{p}\mathbf{y}^2 = \mathbf{y}^1 + \frac{\Delta t}{2}\ \left(3\ \mathbf{F}^1 - \mathbf{F}^0\right) \tag{4.15} $$

7. The predicted solution is corrected by using the *Adams-Moulton Two-Step Method*

$$ {}^{k+1}\mathbf{y}^2 = \mathbf{y}^1 + \frac{\Delta t}{12}\ \left(5\ {}^{k}\mathbf{F}^2 + 8\ \mathbf{F}^1 - \mathbf{F}^0\right) \tag{4.16} $$

where

$$ {}^{k}\mathbf{F}^2 = \mathbf{F}\left({}^{k}\mathbf{y}^2\right) \tag{4.17} $$

and ${}^{1}\mathbf{y}^2 = {}^{p}\mathbf{y}^2$.

8. The previous step is repeatedly applied until the iteration error

$$ e^2 = \left\| {}^{k+1}\mathbf{y}^2 - {}^{k}\mathbf{y}^2 \right\|_{\infty} \tag{4.18} $$

is less than the prescribed error tolerance ϵ.
If $e^2 > \epsilon$ then we set

$$ {}^{k}\mathbf{y}^2 = {}^{k+1}\mathbf{y}^2 \tag{4.19} $$

$$ {}^{k}\dot{\mathbf{y}}^2 = {}^{k+1}\dot{\mathbf{y}}^2 \tag{4.20} $$

and go to Equation (4.16); if $e^2 \leq \epsilon$ then we set

$$ \mathbf{y}^2 = {}^{k+1}\mathbf{y}^2 \tag{4.21} $$

$$ \dot{\mathbf{y}}^2 = {}^{k+1}\dot{\mathbf{y}}^2 \tag{4.22} $$

and compute the response at $t_3 = t_2 + \Delta t$.

9. At t_3 (i.e., $t = 3\Delta t$) the *predicted* solution, ${}^{p}\mathbf{y}^3$, is computed by the *Adams-Bashforth*

Three-Step Predictor Method

$$ {}^{p}\mathbf{y}^3 = \mathbf{y}^2 + \frac{\Delta t}{12} \left(23\ \mathbf{F}^2 - 16\ \mathbf{F}^1 + 5\ \mathbf{F}^0\right) \tag{4.23} $$

10. The predicted solution is corrected by using the *Adams-Moulton Three-Step Method*

$$ {}^{k+1}\mathbf{y}^3 = \mathbf{y}^2 + \frac{\Delta t}{24} \left(9\ {}^{k}\mathbf{F}^3 + 19\ \mathbf{F}^2 - 5\ \mathbf{F}^1 + \mathbf{F}^0\right) \tag{4.24} $$

where

$$ {}^{k}\mathbf{F}^3 = \mathbf{F}\left({}^{k}\mathbf{y}^3\right) \tag{4.25} $$

and ${}^{1}\mathbf{y}^3 = {}^{p}\mathbf{y}^3$.

11. The previous step is repeatedly applied until the iteration error

$$ e^3 = \left\| {}^{k+1}\mathbf{y}^3 - {}^{k}\mathbf{y}^3 \right\|_\infty \tag{4.26} $$

is less than the prescribed error tolerance ϵ.

If $e^3 > \epsilon$ then we set

$$ {}^{k}\mathbf{y}^3 = {}^{k+1}\mathbf{y}^3 \tag{4.27} $$

$$ {}^{k}\dot{\mathbf{y}}^3 = {}^{k+1}\dot{\mathbf{y}}^3 \tag{4.28} $$

and go to Equation (4.24); if $e^3 \leq \epsilon$ then for the first time we evaluate the *Local Truncation Error*

$$ \mathbf{e}^3 = {}^{k+1}\mathbf{y}^3 - {}^{1}\mathbf{y}^3 \tag{4.29} $$

set

$$ \mathbf{y}^3 = {}^{k+1}\mathbf{y}^3 \tag{4.30} $$

$$ \dot{\mathbf{y}}^3 = {}^{k+1}\dot{\mathbf{y}}^3 \tag{4.31} $$

and compute the response at $t_4 = t_3 + \Delta t$.

12. For $t_4, t_5, t_6, \ldots$ (i.e., $t = 4\Delta t, 5\Delta t, 6\Delta t, \ldots$) the solution is computed by using *Hamming's Fourth-Order Modified Predictor-Corrector Method*. The *predicted* solution, ${}^{p}\mathbf{y}^{j}$, is calculated by the *Predictor Equation*

$$ {}^{p}\mathbf{y}^{j} = \mathbf{y}^{j-4} + \frac{4}{3}\Delta t \ \left(2\ \mathbf{F}^{j-1} - \mathbf{F}^{j-2} + 2\ \mathbf{F}^{j-3}\right) \tag{4.32} $$

13. The predicted solution is modified by using the local truncation error from the previous time step

$$ {}^{1}\mathbf{y}^{j} = \ {}^{p}\mathbf{y}^{j} + \frac{112}{9}\ \mathbf{e}^{j-1} \tag{4.33} $$

14. The *modified-predicted* solution is corrected by using the *Corrector Equation*

$$ {}^{k+1}\mathbf{y}^{j} = \frac{1}{8}\left[9\ \mathbf{y}^{j-1} - \mathbf{y}^{j-3} + 3\Delta t\ \left(\ {}^{k}\mathbf{F}^{j} + 2\ \mathbf{F}^{j-1} - \mathbf{F}^{j-2}\right)\right] \tag{4.34} $$

where

$$ {}^{k}\mathbf{F}^{j} = \mathbf{F}\left({}^{k}\mathbf{y}^{j}\right) \tag{4.35} $$

and ${}^{1}\mathbf{y}^{j} = \ {}^{p}\mathbf{y}^{j}$.

15. The previous step is repeatedly applied until the iteration error

$$ e^{j} = \left\| \ {}^{k+1}\mathbf{y}^{j} - \ {}^{k}\mathbf{y}^{j} \right\|_{\infty} \tag{4.36} $$

is less than the prescribed error tolerance ϵ.

16. The local truncation error is estimated for use in the current and next time steps

$$ \mathbf{e}^{j} = \frac{9}{121}\left(\ {}^{k+1}\mathbf{y}^{j} - \ {}^{p}\mathbf{y}^{j}\right) \tag{4.37} $$

17. The *final solution* at step j is

$$ \mathbf{y}^{j} = \ {}^{k+1}\mathbf{y}^{j} - \mathbf{e}^{j} \tag{4.38} $$

18. To calculate the solution at the next time step, we set

$$\mathbf{y}^{j-4} = \mathbf{y}^{j-3} \tag{4.39}$$

$$\mathbf{y}^{j-3} = \mathbf{y}^{j-2} \tag{4.40}$$

$$\mathbf{y}^{j-2} = \mathbf{y}^{j-1} \tag{4.41}$$

$$\mathbf{y}^{j-1} = \mathbf{y}^{j} \tag{4.42}$$

$$\mathbf{e}^{j-1} = \mathbf{e}^{j} \tag{4.43}$$

and go to step (4.32). One can repeat steps (4.32)-(4.43) as much as desired.

4.2 Integrating the Aerodynamic Model into the Numerical Scheme

During a time step Δt, the wakes convect to their new positions consistent with the requirement that vorticity moves with the fluid particles while simultaneously the structures move to their new positions consistent with the current forces, equations of motion, and control law. This concept is implemented by performing the following sequence of steps to calculate the solution at time $= t + \Delta t$ when the solution is known at time $= t$, $t - \Delta t$, $t - 2\Delta t$, and $t - 3\Delta t$:

1. The wakes are convected to their new positions. A fluid particle in a wake is moved to its new position $\mathbf{R}(t + \Delta t)$ from its current position $\mathbf{R}(t)$ according to

$$\mathbf{R}(t + \Delta t) = \mathbf{R}(t) + \mathbf{V}[\mathbf{R}(t)]\ \Delta t \tag{4.44}$$

   During the remainder of the procedure for this time step the wake is not moved. Numerical experiments with more accurate algorithms for convecting the wake have shown that this one is adequate; these have included iterative procedures that use the velocity of the wake in its final position.

2. The current loads (i.e., those at the beginning of the time step when time $= t$) are used to "predict" the state of the structure and, when controls are being used, the current state

is used to reposition the wing relative to the bridge. The predicted solution is given by Equation (4.32).

3. The predicted solution is "modified" by the local truncation error from the previous time step, Equation (4.33).

4. The modified–predicted solution is "corrected" by the iterative procedure which makes use of the corrector equation (4.34). The loads are recalculated for each iteration, but as stated above the wake is not moved. For the elastic loads this is a small effort, but for the aerodynamic loads, the aerodynamic model must be used to recalculate the flowfield. This step is repeated until there is convergence; i.e., until the iteration error given by Equation (4.36) is below a user-specified value. Usually two to four iterations are required to reduce the iteration error to 10^{-6}.

5. After convergence, the local truncation error given by Equation (4.37) is obtained for the next time step and for the final evaluation of the loads at the current time step.

6. Then, Equation (4.38) is used to evaluate the final position and velocity of the structure, and these are used to recalculate the flowfield and to obtain the final estimate of the aerodynamic loads.

At this point the position and velocity of the structure, the distribution of the vorticity and the aerodynamic loads on the lifting surfaces, and the distribution of vorticity in as well as the position of the wakes are known at time $= t + \Delta t$. We are ready to calculate the solution at the next time step. We begin by shifting the information according to Equations (4.39)-(4.43) and then we repeat the steps of this section.

The procedure described above needs information from four time steps. At the beginning, this information does not exist so we use a special starting scheme, which is part of the description in Section 4.1.

At $t = 0$, we use the initial conditions to calculate the aerodynamic loads ignoring the contribution of $\frac{\partial \Phi}{\partial t}$. It is not important to capture this contribution accurately at this step because we are determining the response of the structure to an arbitrary initial disturbance.

Then we use Equation (4.5) to calculate $\mathbf{F}^0$ and we convect the wake to its position at the next time step.

Next we predict the state of the structure at time $= \Delta t$ using the first-order Euler Method given by Equation (4.6). Then we iteratively correct the predicted state using the Modified Euler Method given by Equation (4.7), re-calculating the loads at every iteration. As stated above, we do not recalculate the position of the wake.

After convergence, we advance the time and convect the wakes. Then we predict the solution at time $= 2\Delta t$ using the second-order Adams-Bashforth Two-Step Predictor Method given by Equation (4.15). Next we iteratively correct the predicted solution using the Adams-Moulton Two-Step Method given by Equation (4.16), re-calculating the loads at every iteration.

After convergence, we advance the time and convect the wakes. Then we predict the solution at time $= 3\Delta t$ using the third-order Adams-Bashforth Three-Step Predictor Method given by Equation (4.23). Next we iteratively correct the predicted solution using the Adams-Moulton Three-Step Method given by Equation (4.24), re-calculating the loads at every iteration.

After convergence, we calculate the local truncation error for the first time and then follow the general procedure described at the beginning of this section.

4.3 Bridge One

The equations of motion for bridge one are given by Equations (3.35) and (3.36), which for convenience are repeated below:

$$\ddot{y}(t) = -\alpha_1\, y(t) - \alpha_2\, y(t)^2 - \alpha_3\, y(t)^3 + D_1\, Q_y$$

$$\ddot{\theta}(t) = -\beta_1\, \theta(t) - \beta_2\, \theta(t)^2 - \beta_3\, \theta(t)^3 + D_2\, Q_\theta$$

The first step in the scheme to integrate Equations (3.35) and (3.36) is to rewrite them as a system of first order equations. To this end we introduce the state variables $y_1(t)$, $y_2(t)$, $y_2(t)$, and $y_4(t)$:

$$y_1(t) = y(t)\,, \quad y_2(t) = \theta(t)\,, \quad y_3(t) = \dot{y}(t)\,, \text{ and } \; y_4(t) = \dot{\theta}(t) \qquad (4.45)$$

hence, Equations (3.35) and (3.36) can be rewritten as follows

$$\left\{ \begin{array}{c} \dot{y}_1(t) \\ \dot{y}_2(t) \\ \dot{y}_3(t) \\ \dot{y}_4(t) \end{array} \right\} = \left\{ \begin{array}{c} y_3(t) \\ y_4(t) \\ -\alpha_1\ y_1(t) - \alpha_2\ y_1(t)^2 - \alpha_3\ y_1(t)^3 + D_1\ Q_y[\mathbf{y}(t)] \\ -\beta_1\ \ y_2(t) - \beta_2\ y_2(t)^2 - \beta_3\ y_2(t)^3 + D_2\ Q_\theta[\mathbf{y}(t)] \end{array} \right\} \tag{4.46}$$

or

$$\dot{\mathbf{y}}(t) = \mathbf{F}[\mathbf{y}(t)] \tag{4.47}$$

Equation (4.47) is integrated by using the numerical integration scheme discussed in Sections 4.1 and 4.2.

4.4 Bridge Two

The equations of motion for bridge two are given by Equations (3.44) and (3.45), which for convenience are repeated below:

$$\begin{aligned} \ddot{y}(t) &= -\omega_1^2\ y(t) + D_1\ Q_y \\ \ddot{\theta}(t) &= -\omega_2^2\ \theta(t) - D_2\ Q_\theta \end{aligned}$$

The first step in the scheme to integrate Equations (3.44) and (3.45) is to rewrite them as a system of first order equations. To this end we introduce the state variables $y_1(t)$, $y_2(t)$, $y_2(t)$, and $y_4(t)$:

$$y_1(t) = y(t)\,,\ \ y_2(t) = \theta(t)\,,\ \ y_3(t) = \dot{y}(t)\,,\ \mathit{and}\ y_4(t) = \dot{\theta}(t) \tag{4.48}$$

hence, Equations (3.44) and (3.45) can be rewritten in state form as

$$\left\{ \begin{array}{c} \dot{y}_1(t) \\ \dot{y}_2(t) \\ \dot{y}_3(t) \\ \dot{y}_4(t) \end{array} \right\} = \left[\begin{array}{cccc} 0 & 0 & 1 & 0 \\ 0 & 0 & 0 & 1 \\ -\omega_1^2 & 0 & 0 & 0 \\ 0 & -\omega_2^2 & 0 & 0 \end{array} \right] \left\{ \begin{array}{c} y_1(t) \\ y_2(t) \\ y_3(t) \\ y_4(t) \end{array} \right\} + \left\{ \begin{array}{c} 0 \\ 0 \\ D_1\ Q_y[\mathbf{y}(t)] \\ D_2\ Q_\theta[\mathbf{y}(t)] \end{array} \right\} \tag{4.49}$$

or

$$\dot{\mathbf{y}}\,(t) = \mathbf{A}\ \mathbf{y}\,(t) + \mathbf{b} = \mathbf{F}\,[\mathbf{y}\,(t)] \tag{4.50}$$

Equation (4.50) is integrated by using the numerical integration scheme discussed in Sections 4.1 and 4.2.

4.5 Wing

An essential element of any aeroelastic simulation is the transfer of forces from the aerodynamic grid to the structural grid and of displacements from the structural grid to the aerodynamic grid. In this section, we describe the method used in the present analysis. We relate the *displacements of arbitrary points in the aerodynamic grid* to the *generalized structural nodal displacements* through the following linear transformation:

$$\mathbf{U}_A^*\,(t^*) = [\mathbf{G}_{AS}^*]\ \ \mathbf{V}_S^*\,(t^*) \tag{4.51}$$

where $\mathbf{U}_A^*\,(t)$ is a $(3n_A \times 1)$ vector containing the components of the displacements of the selected points in the aerodynamic grid, $\mathbf{V}_S^*\,(t^*)$ is a $(6n_S \times 1)$ vector containing the components of the generalized structural nodal displacements, n_A is the number of selected points in the aerodynamic grid, n_S is the number of nodes in the structural grid, and $[\mathbf{G}_{AS}^*]$ is the $(3n_A \times 6n_S)$ "interpolation" matrix that relates the generalized displacements of the nodal points in the structural grid to the displacements of the selected points in the aerodynamic grid. $[\mathbf{G}_{AS}^*]$ depends on (1) the geometry of both the aerodynamic and structural grids, (2) the particular points selected in the aerodynamic grid, and (3) the particular kind of finite element selected to discretize the structure.

As an example we describe the matrix $[\mathbf{G}_{AS}^*]$ that relates the displacements of the nodes of the aerodynamic grid to those of the structural grid for the simple case represented in Figure 4-1. The number of aerodynamic nodes is 15; thus, $n_A = 15$. The number of structural nodes is $n_s = 5$. Equation (4.51) has the following expanded form:

$$
\begin{Bmatrix} \mathbf{U}_1^*(t^*) \\ \mathbf{U}_2^*(t^*) \\ \mathbf{U}_3^*(t^*) \\ \mathbf{U}_4^*(t^*) \\ \mathbf{U}_5^*(t^*) \\ \mathbf{U}_6^*(t^*) \\ \mathbf{U}_7^*(t^*) \\ \mathbf{U}_8^*(t^*) \\ \mathbf{U}_9^*(t^*) \\ \mathbf{U}_{10}^*(t^*) \\ \mathbf{U}_{11}^*(t^*) \\ \mathbf{U}_{12}^*(t^*) \\ \mathbf{U}_{13}^*(t^*) \\ \mathbf{U}_{14}^*(t^*) \\ \mathbf{U}_{15}^*(t^*) \end{Bmatrix}_A = \begin{bmatrix} \mathbf{0} & \mathbf{0} & \mathbf{0} & \mathbf{0} & \mathbf{0} \\ \mathbf{G}^*_{AS_{2,1}} & \mathbf{G}^*_{AS_{2,2}} & \mathbf{0} & \mathbf{0} & \mathbf{0} \\ \mathbf{0} & \mathbf{G}^*_{AS_{3,2}} & \mathbf{G}^*_{AS_{3,3}} & \mathbf{0} & \mathbf{0} \\ \mathbf{0} & \mathbf{0} & \mathbf{0} & \mathbf{G}^*_{AS_{4,4}} & \mathbf{G}^*_{AS_{4,5}} \\ \mathbf{0} & \mathbf{0} & \mathbf{0} & \mathbf{0} & \mathbf{G}^*_{AS_{5,5}} \\ \mathbf{0} & \mathbf{0} & \mathbf{0} & \mathbf{0} & \mathbf{0} \\ \mathbf{0} & \mathbf{G}^*_{AS_{7,2}} & \mathbf{G}^*_{AS_{7,3}} & \mathbf{0} & \mathbf{0} \\ \mathbf{0} & \mathbf{0} & \mathbf{G}^*_{AS_{8,3}} & \mathbf{G}^*_{AS_{8,4}} & \mathbf{0} \\ \mathbf{0} & \mathbf{0} & \mathbf{0} & \mathbf{G}^*_{AS_{9,4}} & \mathbf{G}^*_{AS_{9,5}} \\ \mathbf{0} & \mathbf{0} & \mathbf{0} & \mathbf{0} & \mathbf{G}^*_{AS_{10,5}} \\ \mathbf{0} & \mathbf{0} & \mathbf{0} & \mathbf{0} & \mathbf{0} \\ \mathbf{0} & \mathbf{G}^*_{AS_{12,2}} & \mathbf{G}^*_{AS_{12,3}} & \mathbf{0} & \mathbf{0} \\ \mathbf{0} & \mathbf{0} & \mathbf{G}^*_{AS_{13,3}} & \mathbf{G}^*_{AS_{13,4}} & \mathbf{0} \\ \mathbf{0} & \mathbf{0} & \mathbf{0} & \mathbf{G}^*_{AS_{14,4}} & \mathbf{G}^*_{AS_{14,5}} \\ \mathbf{0} & \mathbf{0} & \mathbf{0} & \mathbf{0} & \mathbf{G}^*_{AS_{15,5}} \end{bmatrix} \begin{Bmatrix} \mathbf{V}_1^*(t^*) \\ \mathbf{V}_2^*(t^*) \\ \mathbf{V}_3^*(t^*) \\ \mathbf{V}_4^*(t^*) \\ \mathbf{V}_5^*(t^*) \end{Bmatrix}_S \tag{4.52}
$$

where $\{\mathbf{U}_i^*(t^*)\}_A$ is a (3×1) vector listing the three translations of the i-th aerodynamic node, $\left\{\mathbf{V}_j^*(t^*)\right\}_S = \begin{Bmatrix} \mathbf{U}_j^*(t^*) \\ \mathbf{\Theta}_j(t^*) \end{Bmatrix}_S$ is a (6×1) vector listing the three translations, $\{\mathbf{U}_j(t^*)\}_S$, and the three rotations, $\{\mathbf{\Theta}_j(t^*)\}_S$, of the j-th structural node, $\left[\mathbf{G}^*_{AS_{m,n}}\right]$ is a (3×6) matrix that relates the displacements of the m-th aerodynamic node with the generalized displacements of the n-th structural node, and $\mathbf{0}$ is a (3×6) matrix of zeros. The top row of $[\mathbf{G}^*_{AS}]$ is zero because of the boundary conditions. The derivation of the elements of these matrices is discussed in Section 4.5.2.

To relate the structural forces $\mathbf{F}^*_S$ to the aerodynamic forces $\mathbf{F}^*_A$, we require that the two systems of forces be structurally equivalent. By structurally equivalent we mean that the two force systems will do the same work for any virtual displacement, i.e.,

$$
\delta \bar{W}^*_A = \delta \bar{W}^*_S \tag{4.53}
$$

where the bar over δW_A^* and δW_S^* indicates that these quantities represent infinitesimal increments, not true variations; the virtual work is given by

$$\delta \bar{W}_A^* = \left(\delta \mathbf{U}_A^*\right)^T \ \mathbf{F}_A^* \quad \text{and} \quad \delta \bar{W}_S^* = \left(\delta \mathbf{V}_S^*\right)^T \ \mathbf{F}_S^* \tag{4.54}$$

$\delta \bar{W}_A^*$ is the virtual work performed by the aerodynamic forces over the virtual displacement $\delta \mathbf{U}_A^*$, and $\delta \bar{W}_S^*$ is the virtual work performed by the structural forces over the virtual displacement $\delta \mathbf{V}_S^*$.

Having already decided how the displacement fields of the two grids are related, we can use Equation (4.51) to relate the virtual displacements in the aerodynamic grid to those in the structural grid as follows:

$$\delta \mathbf{U}_A^{CP*} = \left[\mathbf{G}_{AS}^{CP*}\right] \ \delta \mathbf{V}_S^* \tag{4.55}$$

where the superscript CP indicates that the selected points used to develop $[\mathbf{G}_{AS}^*]$ in this application are the control points.

Then the requirement that the work done by the two force systems be equal leads to

$$\begin{aligned} \delta \bar{W}_A^* &= \left(\delta \mathbf{U}_A^{CP*}\right)^T \ \mathbf{F}_A^* = \left(\delta \mathbf{V}_S^*\right)^T \ \left[\mathbf{G}_{AS}^{CP*}\right]^T \mathbf{F}_A^* && (4.56) \\ &= \delta \bar{W}_S^* = \left(\delta \mathbf{V}_S^*\right)^T \ \mathbf{F}_S^* && (4.57) \end{aligned}$$

and because of the arbitrariness of the virtual displacements $\delta \mathbf{V}_S^*$

$$\begin{aligned} \mathbf{F}_S^* &= \left[\mathbf{G}_{AS}^{CP*}\right]^T \ \mathbf{F}_A^* && (4.58) \\ &= \left[\mathbf{G}_{SA}^{CP*}\right] \ \mathbf{F}_A^* && (4.59) \end{aligned}$$

Substituting the expression for $\mathbf{F}_S^*$ given by Equation (4.59) into the equation of motion for the wing, Equation (3.26), which for convenience is repeated here:

$$\ddot{\mathbf{q}}(t) + [\mathbf{\Lambda}] \ \mathbf{q}(t) = T_C^2 \ \mathrm{diag}\left(m_j^*\right)^{-1} [\mathbf{\Phi}^*]^T \ \mathbf{F}_S^*(t^*)$$

gives

$$\ddot{\mathbf{q}}\,(t) + [\mathbf{\Lambda}]\ \mathbf{q}\,(t) = T_C^2\ \text{diag}\left(m_j^*\right)^{-1} [\mathbf{\Phi}^*]^T\ \left[\mathbf{G}_{SA}^{CP*}\right]\ \mathbf{F}_A^* \tag{4.60}$$

We define a new matrix $\left[\mathbf{G}_{MA}^{CP*}\right]$ to relate the aerodynamic forces to the modal forces:

$$\left[\mathbf{G}_{MA}^{CP*}\right] = \left\{\left[\mathbf{G}_{AS}^{CP*}\right][\mathbf{\Phi}^*]\,\text{diag}\left(m_j^*\right)^{-1}\right\}^T \tag{4.61}$$

Equation (4.60) can be rewritten as follows

$$\ddot{\mathbf{q}}\,(t) + [\mathbf{\Lambda}]\ \mathbf{q}\,(t) = T_C^2\ \left[\mathbf{G}_{MA}^{CP*}\right]\ \mathbf{F}_A^* \tag{4.62}$$

4.5.1 The Dimensionless Form of $\mathbf{F}_A^*$

We consider next the aerodynamic force $\{\mathbf{F}_k^*\}_A$ acting on panel k. This force is considered to be applied at the control point and is given by

$$\{\mathbf{F}_k^*\}_A = \Delta p_k^*\ A_k^*\ \hat{\mathbf{n}}_k \tag{4.63}$$

where $\Delta p_k^* = (p_L^*)_k - (p_U^*)_k$ is the pressure jump across the panel at the control point k, and is defined as the pressure below the panel (point L) minus the pressure above the panel (point U). This pressure jump is found from Bernoulli's equation for unsteady flows, Equation (2.76), as described in Chapter 2. A_k^* is the area of panel k, and $\hat{\mathbf{n}}_k$ is the unit vector normal to panel k.

Making use of the definition of the pressure coefficient C_p, given by Equation (2.83), we can write the pressure jump as follows:

$$\Delta p_k^* = (\Delta C_p)_k\ \frac{1}{2}\rho_C V_C^2 \tag{4.64}$$

and using the characteristic length L_C, we can write the area of the panel A_k^* in terms of the dimensionless area A_k as

$$A_k^* = L_C^2\ A_k \tag{4.65}$$

Introducing Equations (4.64) and (4.65) into Equation (4.63), we obtain

$$\{\mathbf{F}_k^*\}_A = \frac{1}{2}\rho_C V_C^2 L_C^2 \ (\Delta C_p)_k \ A_k \ \hat{\mathbf{n}}_k \tag{4.66}$$

We define the *dimensionless aerodynamic force* $\{\mathbf{F}_k\}_A$ as

$$\{\mathbf{F}_k\}_A = (\Delta C_p)_k \ A_k \ \hat{\mathbf{n}}_k \tag{4.67}$$

and rewrite Equation (4.66) as

$$\{\mathbf{F}_k^*\}_A = \frac{1}{2}\rho_C V_C^2 L_C^2 \ \{\mathbf{F}_k\}_A \tag{4.68}$$

By extending this idea to all the panels that form the aerodynamic mesh we have

$$\mathbf{F}_A^* = \left\{\begin{array}{c} \mathbf{F}_1^* \\ \mathbf{F}_2^* \\ \vdots \\ \mathbf{F}_{NP}^* \end{array}\right\}_A = \frac{1}{2}\rho_C V_C^2 L_C^2 \left\{\begin{array}{c} \mathbf{F}_1 \\ \mathbf{F}_2 \\ \vdots \\ \mathbf{F}_{NP} \end{array}\right\}_A \tag{4.69}$$

$$= \left(\frac{1}{2}\rho_C V_C^2 L_C^2\right) \ \mathbf{F}_A \tag{4.70}$$

where NP is the number of panels in the aerodynamic mesh.

Then, substituting the expression for $\mathbf{F}_A^*$ given by Equation (4.70) into the equation of motion of the wing, Equation (4.62), we obtain

$$\ddot{\mathbf{q}}(t) + [\mathbf{\Lambda}] \ \mathbf{q}(t) = T_C^2 \ \left[\mathbf{G}_{MA}^{CP*}\right] \ \left(\frac{1}{2}\rho_C V_C^2 L_C^2\right) \ \mathbf{F}_A \tag{4.71}$$

and, taking into account that $L_C = V_C T_C$ we can write

$$\ddot{\mathbf{q}}(t) + [\mathbf{\Lambda}] \ \mathbf{q}(t) = \left(\frac{1}{2}\rho_C L_C^4\right) \left[\mathbf{G}_{MA}^{CP*}\right] \ \ \mathbf{F}_A \tag{4.72}$$

4.5.2 The Matrix $[\mathbf{G}_{AS}^*]$

In this section we discuss how the individual blocks that comprise $[\mathbf{G}_{AS}^*]$ are constructed. Each block relates the translations of a selected point on the aerodynamic grid, point B, to the generalized displacements of the appropriate nodal points on the structural grid. In developing these blocks we consider point B to lie in a plane perpendicular to the undeformed elastic-axis. There are two cases: (1) the plane containing point B intersects the elastic-axis, and (2) this plane intersects an extension of the elastic-axis. They are discussed individually in the next two subsections.

Case I: Connection to an Internal Point

We select point B on the aerodynamic grid and then find point A on the elastic-axis between the structural nodes I and J such that A and B lie in same plane perpendicular to the undeformed elastic-axis. The cross section of the wing that contains points A and B is assumed to be rigid. The position of point B relative to point A is given by the vector $\mathbf{r}^*$; see Figure 4-2. For this case, the displacement of point B is related to the generalized displacements of point A by the following expression

$$\mathbf{u}_B^* = \left[\begin{array}{c|c} \mathbf{I}_{3\times3} & \mathbf{T}_1 \end{array} \right] \left\{ \begin{array}{c} \mathbf{u}_A^* \\ \boldsymbol{\theta}_A \end{array} \right\} \tag{4.73}$$

or

$$\left\{ \begin{array}{c} u_1^* \\ u_2^* \\ u_3^* \end{array} \right\}_B = \left[\begin{array}{ccc|ccc} 1 & 0 & 0 & 0 & r_3^* & 0 \\ 0 & 1 & 0 & -r_3^* & 0 & r_1^* \\ 0 & 0 & 1 & 0 & -r_1^* & 0 \end{array} \right] \left\{ \begin{array}{c} u_1^* \\ u_2^* \\ u_3^* \\ \theta_1 \\ \theta_2 \\ \theta_3 \end{array} \right\}_A \tag{4.74}$$

where (r_1^*, r_2^*, r_3^*) are the components of the vector $\mathbf{r}^*$, $(u_1^*, u_2^*, u_3^*)_B$ are the components of the translation of point B on the aerodynamic grid, and $(u_1^*, u_2^*, u_3^*, \theta_1, \theta_2, \theta_2)_A$ are the components of the generalized displacement of point A on the structural grid; all components are expressed in the elastic-axis coordinate system.

Using the characteristic length L_C, we can rewrite $\mathbf{r}^*$ as follows

$$\mathbf{r}^* = L_C \; \mathbf{r} \tag{4.75}$$

and Equation (4.74) becomes

$$\left\{\begin{array}{c} u_1^* \\ u_2^* \\ u_3^* \end{array}\right\}_B = \left[\begin{array}{ccc|ccc} 1 & 0 & 0 & 0 & L_C\ r_3 & 0 \\ 0 & 1 & 0 & -L_C\ r_3 & 0 & L_C\ r_1 \\ 0 & 0 & 1 & 0 & -L_C\ r_1 & 0 \end{array}\right] \left\{\begin{array}{c} u_1^* \\ u_2^* \\ u_3^* \\ \theta_1 \\ \theta_2 \\ \theta_3 \end{array}\right\}_A \tag{4.76}$$

The displacement field inside each finite element depends on the particular kind of finite element selected in the process of discretization. In general, these fields may be written as linear combinations of the shape functions and the nodal displacements. For the particular finite element used in this work, "CBAR", the displacement/rotation fields are a linear combination of shape the functions $\bar{N}_1$ through $\bar{N}_6$, the displacements u_i^{I*} and u_i^{J*} as well as the rotations θ_i^I and θ_i^J of the nodal points I and J as follows:

$$\begin{aligned} u_1^*(\eta^*) &= u_1^{I*}\ \bar{N}_3(\eta^*; h_e^*) + u_1^{J*}\ \bar{N}_4(\eta^*; h_e^*) \\ &- \theta_3^I\ \bar{N}_5(\eta^*; h_e^*) - \theta_3^J\ \bar{N}_6(\eta^*; h_e^*) \end{aligned} \tag{4.77}$$

$$u_2^*(\eta^*) = u_2^{I*}\ \bar{N}_1(\eta^*; h_e^*) + u_2^{J*}\ \bar{N}_2(\eta^*; h_e^*) \tag{4.78}$$

$$\begin{aligned} u_3^*(\eta^*) &= u_3^{I*}\ \bar{N}_3(\eta^*; h_e^*) + u_3^{J*}\ \bar{N}_4(\eta^*; h_e^*) \\ &+ \theta_1^I\ \bar{N}_5(\eta^*; h_e^*) + \theta_1^J\ \bar{N}_6(\eta^*; h_e^*) \end{aligned} \tag{4.79}$$

and

$$\begin{aligned} \theta_1(\eta^*) &= \frac{d}{d\eta^*} u_3^*(\eta^*) \\ &= u_3^{I*}\ \frac{d}{d\eta^*}\bar{N}_3(\eta^*; h_e^*) + u_3^{J*}\ \frac{d}{d\eta^*}\bar{N}_4(\eta^*; h_e^*) \\ &+ \theta_1^I\ \frac{d}{d\eta^*}\bar{N}_5(\eta^*; h_e^*) + \theta_1^J\ \frac{d}{d\eta^*}\bar{N}_6(\eta^*; h_e^*) \end{aligned} \tag{4.80}$$

$$\theta_2(\eta^*) = \theta_2^I \; \bar{N}_1(\eta^*; h_e^*) + \theta_2^J \; \bar{N}_2(\eta^*; h_e^*) \tag{4.81}$$

$$\begin{aligned} \theta_3(\eta^*) &= -\frac{d}{d\eta^*} u_1^*(\eta^*) \\ &= -u_1^{I*} \frac{d}{d\eta^*} \; \bar{N}_3(\eta^*; h_e^*) - u_1^{J*} \; \frac{d}{d\eta^*} \bar{N}_4(\eta^*; h_e^*) \\ &+ \; \theta_3^I \; \frac{d}{d\eta^*} \bar{N}_5(\eta^*; h_e^*) + \theta_3^J \; \frac{d}{d\eta^*} \bar{N}_6(\eta^*; h_e^*) \end{aligned} \tag{4.82}$$

where

$$\bar{N}_1(\eta^*; h_e^*) = \frac{\eta_J^* - \eta^*}{h_e^*} \tag{4.83}$$

$$\bar{N}_2(\eta^*; h_e^*) = \frac{\eta^* - \eta_I^*}{h_e^*} \tag{4.84}$$

$$\bar{N}_3(\eta^*; h_e^*) = 1 - 3\left(\frac{\eta^* - \eta_I^*}{h_e^*}\right)^2 + 2\left(\frac{\eta^* - \eta_I^*}{h_e^*}\right)^3 \tag{4.85}$$

$$\bar{N}_4(\eta^*; h_e^*) = 3\left(\frac{\eta^* - \eta_I^*}{h_e^*}\right)^2 - 2\left(\frac{\eta^* - \eta_I^*}{h_e^*}\right)^3 \tag{4.86}$$

$$\bar{N}_5(\eta^*; h_e^*) = (\eta^* - \eta_I^*) - \frac{2}{h_e^*}(\eta^* - \eta_I^*)^2 + \frac{1}{h_e^{*2}}(\eta^* - \eta_I^*)^3 \tag{4.87}$$

$$\bar{N}_6(\eta^*; h_e^*) = -\frac{1}{h_e^*}(\eta^* - \eta_I^*)^2 + \frac{1}{h_e^{*2}}(\eta^* - \eta_I^*)^3 \tag{4.88}$$

and

$$\bar{N}_3'(\eta^*; h_e^*) \equiv \frac{d}{d\eta^*}\bar{N}_3(\eta^*; h_e^*) = -\frac{6}{h_e^{*2}}(\eta^* - \eta_I^*) + \frac{1}{h_e^{*3}}(\eta^* - \eta_I^*)^2 \tag{4.89}$$

$$\bar{N}_4'(\eta^*; h_e^*) \equiv \frac{d}{d\eta^*}\bar{N}_4(\eta^*; h_e^*) = \frac{6}{h_e^{*2}}(\eta^* - \eta_I^*) - \frac{6}{h_e^{*3}}(\eta^* - \eta_I^*)^2 \tag{4.90}$$

$$\bar{N}_5'(\eta^*; h_e^*) \equiv \frac{d}{d\eta^*}\bar{N}_5(\eta^*; h_e^*) = 1 - \frac{4}{h_e^*}(\eta^* - \eta_I^*) + \frac{3}{h_e^{*2}}(\eta^* - \eta_I^*)^2 \tag{4.91}$$

$$\bar{N}_6'(\eta^*;h_e^*) \equiv \frac{d}{d\eta^*}\bar{N}_6(\eta^*;h_e^*) = -\frac{2}{h_e^*}(\eta^*-\eta_I^*) + \frac{3}{h_e^{*2}}(\eta^*-\eta_I^*)^2 \tag{4.92}$$

where η_I^* is the coordinate along the elastic-axis of the structural node I, η_J^* is the coordinate along the elastic-axis of the structural node J, and

$$h_e^* = \eta_J^* - \eta_I^* \tag{4.93}$$

is the length between them.

Now, using matrix notation we write the translation $\mathbf{u}_A^*$ and rotation $\boldsymbol{\theta}_A$ of point A, with coordinates $(0,\eta_A^*,0)$ in the elastic-axis system, in terms of the displacements $\mathbf{u}_I^*$ and $\mathbf{u}_J^*$ as well as the rotations $\boldsymbol{\theta}_I$ and $\boldsymbol{\theta}_J$ of the nodal points I and J as follows:

$$\left\{\begin{array}{c}\mathbf{u}_A^*\\ \boldsymbol{\theta}_A\end{array}\right\} = \left[\begin{array}{cc|cc}\bar{\mathbf{N}}_{11} & \bar{\mathbf{N}}_{12} & \bar{\mathbf{N}}_{13} & \bar{\mathbf{N}}_{14}\\ \bar{\mathbf{N}}_{21} & \bar{\mathbf{N}}_{22} & \bar{\mathbf{N}}_{23} & \bar{\mathbf{N}}_{24}\end{array}\right]\left\{\begin{array}{c}\mathbf{u}_I^*\\ \boldsymbol{\theta}_I\\ \hline \mathbf{u}_J^*\\ \boldsymbol{\theta}_J\end{array}\right\} \tag{4.94}$$

where the submatrices $\bar{\mathbf{N}}_{11}$ to $\bar{\mathbf{N}}_{24}$ are given by

$$\bar{\mathbf{N}}_{11} = \begin{bmatrix}\bar{N}_3(\eta_A^*;h_e^*) & 0 & 0\\ 0 & \bar{N}_1(\eta_A^*;h_e^*) & 0\\ 0 & 0 & \bar{N}_3(\eta_A^*;h_e^*)\end{bmatrix} \tag{4.95}$$

$$\bar{\mathbf{N}}_{12} = \begin{bmatrix}0 & 0 & -\bar{N}_5(\eta_A^*;h_e^*)\\ 0 & 0 & 0\\ \bar{N}_5(\eta_A^*;h_e^*) & 0 & 0\end{bmatrix} \tag{4.96}$$

$$\bar{\mathbf{N}}_{13} = \begin{bmatrix}\bar{N}_4(\eta_A^*;h_e^*) & 0 & 0\\ 0 & \bar{N}_2(\eta_A^*;h_e^*) & 0\\ 0 & 0 & \bar{N}_4(\eta_A^*;h_e^*)\end{bmatrix} \tag{4.97}$$

$$\bar{\mathbf{N}}_{14} = \begin{bmatrix} 0 & 0 & -\bar{N}_6\left(\eta_A^*; h_e^*\right) \\ 0 & 0 & 0 \\ \bar{N}_6\left(\eta_A^*; h_e^*\right) & 0 & 0 \end{bmatrix} \tag{4.98}$$

$$\bar{\mathbf{N}}_{21} = \begin{bmatrix} 0 & 0 & \bar{N}_3'\left(\eta_A^*; h_e^*\right) \\ 0 & 0 & 0 \\ -\bar{N}_3'\left(\eta_A^*; h_e^*\right) & 0 & 0 \end{bmatrix} \tag{4.99}$$

$$\bar{\mathbf{N}}_{22} = \begin{bmatrix} \bar{N}_5'\left(\eta_A^*; h_e^*\right) & 0 & 0 \\ 0 & \bar{N}_1\left(\eta_A^*; h_e^*\right) & 0 \\ 0 & 0 & \bar{N}_5'\left(\eta_A^*; h_e^*\right) \end{bmatrix} \tag{4.100}$$

$$\bar{\mathbf{N}}_{23} = \begin{bmatrix} 0 & 0 & \bar{N}_4'\left(\eta_A^*; h_e^*\right) \\ 0 & 0 & 0 \\ -\bar{N}_4'\left(\eta_A^*; h_e^*\right) & 0 & 0 \end{bmatrix} \tag{4.101}$$

$$\bar{\mathbf{N}}_{24} = \begin{bmatrix} \bar{N}_6'\left(\eta_A^*; h_e^*\right) & 0 & 0 \\ 0 & \bar{N}_2\left(\eta_A^*; h_e^*\right) & 0 \\ 0 & 0 & \bar{N}_6'\left(\eta_A^*; h_e^*\right) \end{bmatrix} \tag{4.102}$$

Substituting the expression for $\mathbf{u}_A^*$ and $\boldsymbol{\theta}_A$ given by Equation (4.94) into Equation (4.73), we obtain the following expression for the translation of point B in terms of the displacements $\mathbf{u}_I^*$ and $\mathbf{u}_J^*$ as well as the rotations $\boldsymbol{\theta}_I$ and $\boldsymbol{\theta}_J$ of the nodal points I and J:

$$\mathbf{u}_B^* = \left[\begin{array}{c|c} \mathbf{I}_{3\times 3} & \mathbf{T}_1 \end{array}\right] \left[\begin{array}{cc|cc} \bar{\mathbf{N}}_{11} & \bar{\mathbf{N}}_{12} & \bar{\mathbf{N}}_{13} & \bar{\mathbf{N}}_{14} \\ \bar{\mathbf{N}}_{21} & \bar{\mathbf{N}}_{22} & \bar{\mathbf{N}}_{23} & \bar{\mathbf{N}}_{24} \end{array}\right] \left\{\begin{array}{c} \mathbf{u}_I^* \\ \boldsymbol{\theta}_I \\ \hline \mathbf{u}_J^* \\ \boldsymbol{\theta}_J \end{array}\right\} \tag{4.103}$$

$$= \left[\begin{array}{cc|cc} \mathbf{G}_{AS_1}^* & \mathbf{G}_{AS_2}^* & \mathbf{G}_{AS_3}^* & \mathbf{G}_{AS_4}^* \end{array}\right] \left\{\begin{array}{c} \mathbf{u}_I^* \\ \boldsymbol{\theta}_I \\ \hline \mathbf{u}_J^* \\ \boldsymbol{\theta}_J \end{array}\right\} \tag{4.104}$$

here, the submatrices $\mathbf{G}^*_{AS_1}$ through $\mathbf{G}^*_{AS_1}$ are given by

$$\mathbf{G}^*_{AS_1} = \bar{\mathbf{N}}_{11} + \mathbf{T}_1 \bar{\mathbf{N}}_{21} \tag{4.105}$$

$$= \begin{bmatrix} \bar{N}_3(\eta^*_A; h^*_e) & 0 & 0 \\ -r^*_1 \bar{N}'_3(\eta^*_A; h^*_e) & \bar{N}_1(\eta^*_A; h^*_e) & -r^*_3 \bar{N}'_3(\eta^*_A; h^*_e) \\ 0 & 0 & \bar{N}_3(\eta^*_A; h^*_e) \end{bmatrix} \tag{4.106}$$

$$\mathbf{G}^*_{AS_2} = \bar{\mathbf{N}}_{12} + \mathbf{T}_1 \bar{\mathbf{N}}_{22} \tag{4.107}$$

$$= \begin{bmatrix} 0 & r^*_3 \bar{N}_1(\eta^*_A; h^*_e) & -\bar{N}_5(\eta^*_A; h^*_e) \\ -r^*_3 \bar{N}'_5(\eta^*_A; h^*_e) & 0 & r^*_1 \bar{N}'_5(\eta^*_A; h^*_e) \\ \bar{N}_5(\eta^*_A; h^*_e) & -r^*_1 \bar{N}_1(\eta^*_A; h^*_e) & 0 \end{bmatrix} \tag{4.108}$$

$$\mathbf{G}^*_{AS_3} = \bar{\mathbf{N}}_{13} + \mathbf{T}_1 \bar{\mathbf{N}}_{23} \tag{4.109}$$

$$= \begin{bmatrix} \bar{N}_4(\eta^*_A; h^*_e) & 0 & 0 \\ -r^*_1 \bar{N}'_4(\eta^*_A; h^*_e) & \bar{N}_2(\eta^*_A; h^*_e) & -r^*_3 \bar{N}'_4(\eta^*_A; h^*_e) \\ 0 & 0 & \bar{N}_4(\eta^*_A; h^*_e) \end{bmatrix} \tag{4.110}$$

$$\mathbf{G}^*_{AS_3} = \bar{\mathbf{N}}_{14} + \mathbf{T}_1 \bar{\mathbf{N}}_{24} \tag{4.111}$$

$$= \begin{bmatrix} 0 & r^*_3 \bar{N}_2(\eta^*_A; h^*_e) & -\bar{N}_6(\eta^*_A; h^*_e) \\ -r^*_3 \bar{N}'_6(\eta^*_A; h^*_e) & 0 & r^*_1 \bar{N}'_6(\eta^*_A; h^*_e) \\ \bar{N}_6(\eta^*_A; h^*_e) & -r^*_1 \bar{N}_2(\eta^*_A; h^*_e) & 0 \end{bmatrix} \tag{4.112}$$

At this point it is convenient to introduce dimensionless variables.

Writing Matrix $[\mathbf{G}^*_{AS}]$ in Dimensionless Variables

In order to obtain the dimensionless form of matrix $[\mathbf{G}^*_{AS}]$ we introduce the following dimensionless variables and shape functions:

$$\eta^*(\eta) = L_C\ \eta \tag{4.113}$$

$$h^*_e(h_e) = L_C\ h_e \tag{4.114}$$

$$N_1(\eta; h_e) = \bar{N}_1[\eta^*(\eta); h_e^*(h_e)] \tag{4.115}$$

$$= \frac{\eta_J - \eta}{h_e} \tag{4.116}$$

$$N_2(\eta; h_e) = \bar{N}_2[\eta^*(\eta); h_e^*(h_e)] \tag{4.117}$$

$$= \frac{\eta - \eta_I}{h_e} \tag{4.118}$$

$$N_3(\eta; h_e) = \bar{N}_3[\eta^*(\eta); h_e^*(h_e)] \tag{4.119}$$

$$= 1 - 3\left(\frac{\eta - \eta_I}{h_e}\right)^2 + 2\left(\frac{\eta - \eta_I}{h_e}\right)^3 \tag{4.120}$$

$$N_4(\eta; h_e) = \bar{N}_4[\eta^*(\eta); h_e^*(h_e)] \tag{4.121}$$

$$= 3\left(\frac{\eta - \eta_I}{h_e}\right)^2 - 2\left(\frac{\eta - \eta_I}{h_e}\right)^3 \tag{4.122}$$

$$N_5(\eta; h_e) = \bar{N}_5[\eta^*(\eta); h_e^*(h_e)] \tag{4.123}$$

$$= L_C\left[(\eta - \eta_I) - \frac{2}{h_e}(\eta - \eta_I)^2 + \frac{1}{h_e^2}(\eta - \eta_I)^3\right] \tag{4.124}$$

$$N_6(\eta; h_e) = \bar{N}_6[\eta^*(\eta); h_e^*(h_e)] \tag{4.125}$$

$$= L_C\left[-\frac{1}{h_e}(\eta - \eta_I)^2 + \frac{1}{h_e^2}(\eta - \eta_I)^3\right] \tag{4.126}$$

where L_C is the characteristic length.

The derivatives of the shape functions given by Equations (4.119)-(4.125) with respect to the dimensionless variable η are computed by using the chain rule as follows:

$$\begin{aligned}\frac{d}{d\eta}N_3(\eta; h_e) &= \frac{d}{d\eta^*}\bar{N}_3[\eta^*(\eta); h_e^*(h_e)]\frac{d}{d\eta}\eta^*(\eta)\\ &= L_C\frac{d}{d\eta^*}\bar{N}_3[\eta^*(\eta); h_e^*(h_e)]\end{aligned}$$

$$\begin{aligned}\frac{d}{d\eta}N_4(\eta; h_e) &= \frac{d}{d\eta^*}\bar{N}_4[\eta^*(\eta); h_e^*(h_e)]\frac{d}{d\eta}\eta^*(\eta)\\ &= L_C\frac{d}{d\eta^*}\bar{N}_4[\eta^*(\eta); h_e^*(h_e)]\end{aligned}$$

$$\begin{aligned}\frac{d}{d\eta}N_5(\eta;h_e) &= \frac{d}{d\eta^*}\bar{N}_5\left[\eta^*(\eta);h_e^*(h_e)\right]\frac{d}{d\eta}\eta^*(\eta) \\ &= L_C\frac{d}{d\eta^*}\bar{N}_5\left[\eta^*(\eta);h_e^*(h_e)\right]\end{aligned}$$

$$\begin{aligned}\frac{d}{d\eta}N_6(\eta;h_e) &= \frac{d}{d\eta^*}\bar{N}_6\left[\eta^*(\eta);h_e^*(h_e)\right]\frac{d}{d\eta}\eta^*(\eta) \\ &= L_C\frac{d}{d\eta^*}\bar{N}_6\left[\eta^*(\eta);h_e^*(h_e)\right]\end{aligned}$$

hence, we conclude that

$$\frac{d}{d\eta^*}\bar{N}_3\left[\eta^*(\eta);h_e^*(h_e)\right] = \frac{1}{L_C}\frac{d}{d\eta}N_3(\eta;h_e) \tag{4.127}$$

$$\frac{d}{d\eta^*}\bar{N}_4\left[\eta^*(\eta);h_e^*(h_e)\right] = \frac{1}{L_C}\frac{d}{d\eta}N_4(\eta;h_e) \tag{4.128}$$

$$\frac{d}{d\eta^*}\bar{N}_5\left[\eta^*(\eta);h_e^*(h_e)\right] = \frac{1}{L_C}\frac{d}{d\eta}N_5(\eta;h_e) \tag{4.129}$$

$$\frac{d}{d\eta^*}\bar{N}_6\left[\eta^*(\eta);h_e^*(h_e)\right] = \frac{1}{L_C}\frac{d}{d\eta}N_6(\eta;h_e) \tag{4.130}$$

where

$$N_3'(\eta;h_e) \equiv \frac{d}{d\eta}N_3(\eta;h_e) = -\frac{6}{h_e^2}(\eta-\eta_I)+\frac{6}{h_e^3}(\eta-\eta_I)^2 \tag{4.131}$$

$$N_4'(\eta;h_e) \equiv \frac{d}{d\eta}N_4(\eta;h_e) = \frac{6}{h_e^2}(\eta-\eta_I)-\frac{6}{h_e^3}(\eta-\eta_I)^2 \tag{4.132}$$

$$N_5'(\eta;h_e) \equiv \frac{d}{d\eta}N_5(\eta;h_e) = L_C\left[1-\frac{4}{h_e}(\eta-\eta_I)+\frac{3}{h_e^2}(\eta-\eta_I)^2\right] \tag{4.133}$$

$$N_6'(\eta;h_e) \equiv \frac{d}{d\eta}N_6(\eta;h_e) = L_C\left[-\frac{2}{h_e}(\eta-\eta_I)+\frac{3}{h_e^2}(\eta-\eta_I)^2\right] \tag{4.134}$$

Introducing the expressions for the shape functions $N_1(\eta;h_e)$ through $N_6(\eta;h_e)$, given by

Equations (4.119)-(4.125), and their derivatives, given by Equations (4.131)-(4.134), into Equations (4.105)-(4.111), we can rewrite the components of matrix $[\mathbf{G}^*_{AS}]$ in term of dimensionless variables and the characteristic length as:

$$\mathbf{G}^*_{AS_1} = \bar{\mathbf{N}}_{11} + \mathbf{T}_1\bar{\mathbf{N}}_{21} \tag{4.135}$$

$$= \begin{bmatrix} N_3\left(\eta_A; h_e\right) & 0 & 0 \\ -r_1 N_3'\left(\eta_A; h_e\right) & N_1\left(\eta_A^*; h_e^*\right) & -r_3 N_3'\left(\eta_A; h_e\right) \\ 0 & 0 & N_3\left(\eta_A^*; h_e^*\right) \end{bmatrix} \tag{4.136}$$

$$\mathbf{G}^*_{AS_2} = \bar{\mathbf{N}}_{12} + \mathbf{T}_1\bar{\mathbf{N}}_{22} \tag{4.137}$$

$$= \begin{bmatrix} 0 & L_C r_3 N_1\left(\eta_A; h_e\right) & -N_5\left(\eta_A; h_e\right) \\ -r_3 N_5'\left(\eta_A; h_e\right) & 0 & r_1 N_5'\left(\eta_A; h_e\right) \\ N_5\left(\eta_A; h_e\right) & -r_1 N_1\left(\eta_A; h_e\right) & 0 \end{bmatrix} \tag{4.138}$$

$$\mathbf{G}^*_{AS_3} = \bar{\mathbf{N}}_{13} + \mathbf{T}_1\bar{\mathbf{N}}_{23} \tag{4.139}$$

$$= \begin{bmatrix} N_4\left(\eta_A; h_e\right) & 0 & 0 \\ -r_1 N_4'\left(\eta_A; h_e\right) & N_2\left(\eta_A; h_e\right) & -r_3 N_4'\left(\eta_A; h_e\right) \\ 0 & 0 & N_4\left(\eta_A; h_e\right) \end{bmatrix} \tag{4.140}$$

$$\mathbf{G}^*_{AS_3} = \bar{\mathbf{N}}_{14} + \mathbf{T}_1\bar{\mathbf{N}}_{24} \tag{4.141}$$

$$= \begin{bmatrix} 0 & L_C r_3 N_2\left(\eta_A; h_e\right) & -N_6\left(\eta_A; h_e\right) \\ -r_3 N_6'\left(\eta_A; h_e\right) & 0 & r_1 N_6'\left(\eta_A; h_e\right) \\ N_6\left(\eta_A; h_e\right) & -L_C r_1 N_2\left(\eta_A; h_e\right) & 0 \end{bmatrix} \tag{4.142}$$

Case II: Connection to the End-Point

In this subsection, the plane containing point B intersects an extension of the elastic-axis; point B is near or at the wing-tip (see Figure 4-3). In the figure point N is the last node of the finite element mesh . Point B on the aerodynamic mesh is connected through a rigid link to point N. In this particular case we can write

$$\mathbf{u}_B^* = \left[\begin{array}{c|c} \mathbf{I}_{3\times 3} & \mathbf{T}_2 \end{array} \right] \left\{ \begin{array}{c} \mathbf{u}_N^* \\ \boldsymbol{\theta}_N \end{array} \right\} \tag{4.143}$$

or

$$\left\{ \begin{array}{c} u_1^* \\ u_2^* \\ u_3^* \end{array} \right\}_B = \left[\begin{array}{ccc|ccc} 1 & 0 & 0 & 0 & r_3^* & -r_2^* \\ 0 & 1 & 0 & -r_3^* & 0 & r_1^* \\ 0 & 0 & 1 & r_2^* & -r_1^* & 0 \end{array} \right] \left\{ \begin{array}{c} u_1^* \\ u_2^* \\ u_3^* \\ \theta_1 \\ \theta_2 \\ \theta_3 \end{array} \right\}_N \tag{4.144}$$

where (r_1^*, r_2^*, r_3^*) are the components of the vector $\mathbf{r}^*$, $(u_1^*, u_2^*, u_3^*)_B$ are the components of the translation of point B on the aerodynamic grid, and $(u_1^*, u_2^*, u_3^*, \theta_1, \theta_2, \theta_2)_N$ are the components of the generalized displacement of point N on the structural grid; all components are expressed in the elastic-axis coordinate system. Using the dimensionless expression for $\mathbf{r}^*$ given by Equation (4.75), we can write Equation (4.144) in terms of dimensionless variables and the characteristics length as

$$\left\{ \begin{array}{c} u_1^* \\ u_2^* \\ u_3^* \end{array} \right\}_B = \left[\begin{array}{ccc|ccc} 1 & 0 & 0 & 0 & L_C\ r_3 & -L_C\ r_2 \\ 0 & 1 & 0 & -L_C\ r_3 & 0 & L_C\ r_1 \\ 0 & 0 & 1 & L_C\ r_2 & -L_C\ r_1 & 0 \end{array} \right] \left\{ \begin{array}{c} u_1^* \\ u_2^* \\ u_3^* \\ \theta_1 \\ \theta_2 \\ \theta_3 \end{array} \right\}_N \tag{4.145}$$

or

$$\mathbf{u}_B^* = \left[\begin{array}{cc} \mathbf{G}_{AS_1}^* & \mathbf{G}_{AS_2}^* \end{array} \right] \left\{ \begin{array}{c} \mathbf{u}_N^* \\ \boldsymbol{\theta}_N \end{array} \right\} \tag{4.146}$$

After the procedures explained above are repeated for every selected point in the aerodynamic grid, then we assemble a global matrix $[\mathbf{G}_{AS}^*]$ that maps the generalized displacements of all the structural nodes into the deflections of all the selected points in the aerodynamic grid.

4.5.3 Integration of the Equations of Motion

The first step in the scheme to integrate Equation (4.72) is to rewrite it as a system of first-order equations. To this end we introduce the $(2n \times 1)$ state vector $\mathbf{y}(\mathbf{t}) = \left\{ \begin{array}{c} \mathbf{y}_1(t) \\ \mathbf{y}_2(t) \end{array} \right\}$, where the state variables $\mathbf{y}_1(t)$ and $\mathbf{y}_2(t)$ are given by

$$\mathbf{y}_1(t) = \mathbf{q}(t) \tag{4.147}$$

$$\mathbf{y}_2(t) = \dot{\mathbf{q}}(t) \tag{4.148}$$

Differentiating these equations and using of Equation (4.72) we obtain

$$\dot{\mathbf{y}}_1(t) = \mathbf{y}_2(t) \tag{4.149}$$

$$\dot{\mathbf{y}}_2(t) = -[\mathbf{\Lambda}]\ \mathbf{y}_1(t) + \left(\frac{1}{2}\rho_C L_C^4\right) \left[\mathbf{G}_{MA}^{CP*}\right]\ \ \mathbf{F}_A \tag{4.150}$$

These two sets of equations can now be written in state form as

$$\dot{\mathbf{y}}(t) = [\mathbf{A}]\ \mathbf{y}(t) + \mathbf{b} = \mathbf{F}[\mathbf{y}(t)] \tag{4.151}$$

or

$$\left\{ \begin{array}{c} \dot{\mathbf{y}}_1(t) \\ \hline \dot{\mathbf{y}}_2(t) \end{array} \right\} = \left[\begin{array}{c|c} \mathbf{0}_{n\times n} & \mathbf{I}_{n\times n} \\ \hline -[\mathbf{\Lambda}] & \mathbf{0}_{n\times n} \end{array} \right] \left\{ \begin{array}{c} \mathbf{y}_1(t) \\ \hline \mathbf{y}_2(t) \end{array} \right\} + \left\{ \begin{array}{c} \mathbf{0}_{n\times 1} \\ \hline \left(\frac{1}{2}\rho_C L_C^4\right) \left[\mathbf{G}_{MA}^{CP*}\right]\ \ \mathbf{F}_A \end{array} \right\} \tag{4.152}$$

where $\mathbf{0}_{n\times n}$ is a $(n \times n)$ matrix of zeros, $\mathbf{0}_{n\times 1}$ is a $(n \times 1)$ matrix of zeros, and $\mathbf{I}_{n\times n}$ is the $(n \times n)$ identity matrix. Equation (4.151) is integrated by using the numerical integration scheme discussed in Sections 4.1 and 4.2.

4.5.4 Using $\left[\mathbf{G}_{AS}^{NP*}\right]$ to obtain $\left[\mathbf{G}_{AS}^{CP*}\right]$

We emphasize that two "interpolation" matrices are needed: $\left[\mathbf{G}_{AS}^{NP*}\right]$ to map the generalized displacements and velocities of the structural nodes into the deflections and velocities of the aerodynamic nodes, which are needed for the boundary conditions on the flowfield, and

$\left[\mathbf{G}_{SA}^{CP*}\right] = \left[\mathbf{G}_{AS}^{CP*}\right]^T$ to map the aerodynamic forces into structural nodal forces. As the final topic of this chapter, we discuss how we obtain $\left[\mathbf{G}_{AS}^{CP*}\right]$ from $\left[\mathbf{G}_{AS}^{NP*}\right]$.

In the aerodynamic grid, the number of nodal points (NP) is always greater than the number of control points (CP). For any element in the aerodynamic grid, the position of the control point (both initially and during the motion) is the average of the positions of its corners; see Figure 4-4. This definition is used to compute $\left[\mathbf{G}_{AS}^{CP*}\right]$ from $\left[\mathbf{G}_{AS}^{NP*}\right]$ as follows:

$$\mathbf{u}_p^* = \frac{1}{4}\left(\mathbf{u}_i^* + \mathbf{u}_j^* + \mathbf{u}_k^* + \mathbf{u}_l^*\right) \tag{4.153}$$

or

$$\left\{\begin{array}{c} u_1^{p*} \\ u_2^{p*} \\ u_3^{p*} \end{array}\right\} = \left[\begin{array}{ccc|ccc|ccc|ccc} \frac{1}{4} & 0 & 0 & \frac{1}{4} & 0 & 0 & \frac{1}{4} & 0 & 0 & \frac{1}{4} & 0 & 0 \\ 0 & \frac{1}{4} & 0 & 0 & \frac{1}{4} & 0 & 0 & \frac{1}{4} & 0 & 0 & \frac{1}{4} & 0 \\ 0 & 0 & \frac{1}{4} & 0 & 0 & \frac{1}{4} & 0 & 0 & \frac{1}{4} & 0 & 0 & \frac{1}{4} \end{array}\right] \left\{\begin{array}{c} u_1^{i*} \\ u_2^{i*} \\ u_3^{i*} \\ \hline u_1^{j*} \\ u_2^{j*} \\ u_3^{j*} \\ \hline u_1^{k*} \\ u_2^{k*} \\ u_3^{k*} \\ \hline u_1^{l*} \\ u_2^{l*} \\ u_3^{l*} \end{array}\right\} \tag{4.154}$$

where $\left(u_1^{p*}, u_2^{p*}, u_3^{p*}\right)$ are the components of the translation of the control point p, $\left(u_1^{i*}, u_2^{i*}, u_3^{i*}\right)$, $\left(u_1^{j*}, u_2^{j*}, u_3^{j*}\right)$, $\left(u_1^{k*}, u^{k*}, u_3^{k*}\right)$, and $\left(u_1^{l*}, u_2^{l*}, u_3^{l*}\right)$ are the components of the translation of the aerodynamic nodes i, j, k, and l, respectively; all components are expressed in the elastic-axis coordinate system. Now, using matrix notation we write Equation (4.154) as follows:

$$\mathbf{u}_p^* = [\mathbf{T}_3] \left\{ \begin{array}{c} \mathbf{u}_i^* \\ \hline \mathbf{u}_j^* \\ \hline \mathbf{u}_k^* \\ \hline \mathbf{u}_l^* \end{array} \right\} \tag{4.155}$$

This relationship among the displacement of a control point and the displacements of all four corners is written for every element in the aerodynamic grid. Then we assemble a global matrix $[\mathbf{T}_3]$ that maps the deflection of all nodal points into the deflections of all control points in the aerodynamic grid. Hence, using this global matrix $[\mathbf{T}_3]$ we can write

$$\mathbf{u}_A^{CP*} = [\mathbf{T}_3]\, \mathbf{u}_A^{NP*} \tag{4.156}$$

and taking into account Equation (4.51) we obtain

$$\begin{aligned} \mathbf{u}_A^{CP*} &= [\mathbf{T}_3]\, \mathbf{u}_A^{NP*} \\ &= [\mathbf{T}_3] \left[\mathbf{G}_{AS}^{NP*} \right] \ \mathbf{v}_S^* \\ &= \left[\mathbf{G}_{AS}^{CP*} \right] \ \mathbf{v}_S^* \end{aligned} \tag{4.157}$$

where

$$\left[\mathbf{G}_{AS}^{CP*} \right] = [\mathbf{T}_3] \left[\mathbf{G}_{AS}^{NP*} \right] \tag{4.158}$$

Finally, we note that the displacements of the control points could have been obtained differently by following exactly the same procedure that we used to find the displacements of the aerodynamic nodes.

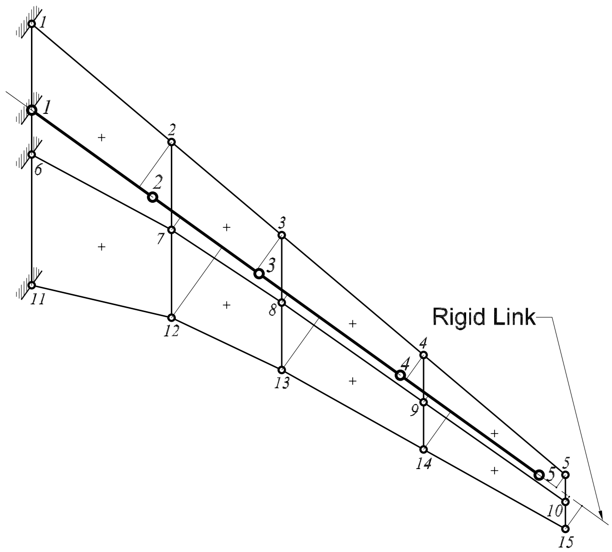

Figure 4-1: Aerodynamic and Structural Grids

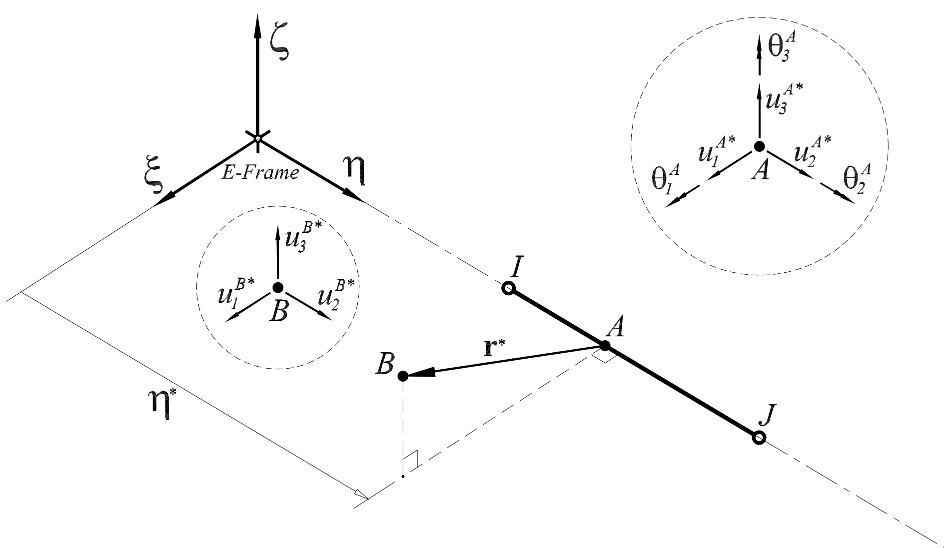

Figure 4-2: Connection to an Internal Point

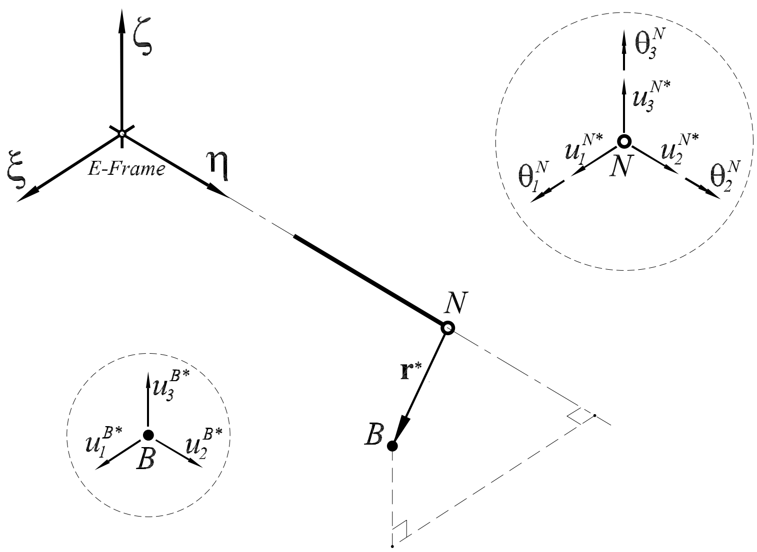

Figure 4-3: Connection to the End-Point

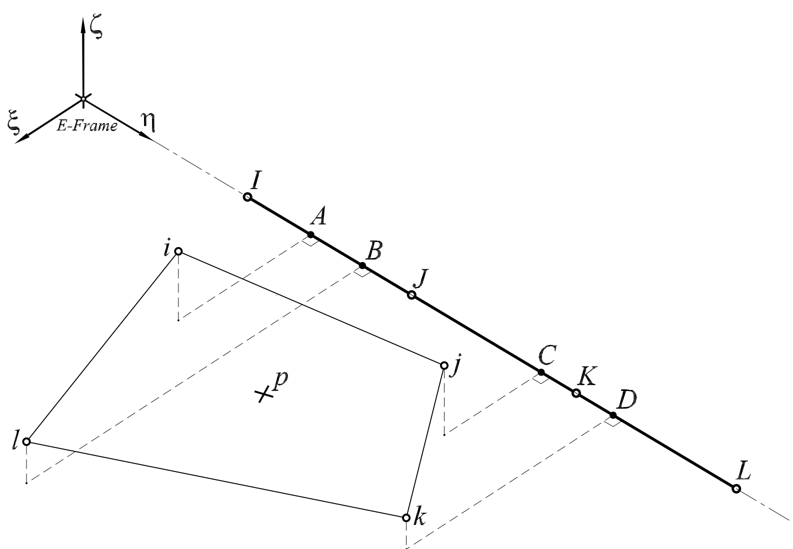

Figure 4-4: Using $\left[\mathbf{G}_{AS}^{NP*}\right]$ to obtain $\left[\mathbf{G}_{AS}^{CP*}\right]$